

Lawrence Berkeley National Laboratory

Recent Work

Title

ENERGY TRANSFER IN ONE-DIMENSIONAL SUBSTITUTIONALLY DISORDERED SYSTEMS. II.
EXPERIMENTAL RESULTS FOR 1,2,4,5,-TETRACHLOROBENZENE

Permalink

<https://escholarship.org/uc/item/3p14h5wf>

Author

Zwemer, D.A.

Publication Date

1978-09-01

ENERGY TRANSFER IN ONE-DIMENSIONAL SUBSTITUTIONALLY
DISORDERED SYSTEMS. II. EXPERIMENTAL RESULTS
FOR 1,2,4,5-TETRACHLOROBENZENE

D. A. Zwemer and C. B. Harris

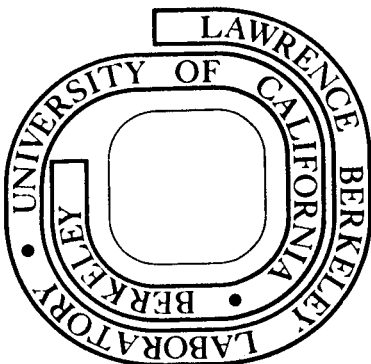
September 1978

Prepared for the U. S. Department of Energy
under Contract W-7405-ENG-48

RECEIVED
LABORATORY

JAN 11 1979

LIBRARY AND
DOCUMENTS SECTION



TWO-WEEK LOAN COPY

*This is a Library Circulating Copy
which may be borrowed for two weeks.
For a personal retention copy, call
Tech. Info. Division, Ext. 6782*

*LBL-8249
c.2*

DISCLAIMER

This document was prepared as an account of work sponsored by the United States Government. While this document is believed to contain correct information, neither the United States Government nor any agency thereof, nor the Regents of the University of California, nor any of their employees, makes any warranty, express or implied, or assumes any legal responsibility for the accuracy, completeness, or usefulness of any information, apparatus, product, or process disclosed, or represents that its use would not infringe privately owned rights. Reference herein to any specific commercial product, process, or service by its trade name, trademark, manufacturer, or otherwise, does not necessarily constitute or imply its endorsement, recommendation, or favoring by the United States Government or any agency thereof, or the Regents of the University of California. The views and opinions of authors expressed herein do not necessarily state or reflect those of the United States Government or any agency thereof or the Regents of the University of California.

ENERGY TRANSFER IN ONE-DIMENSIONAL SUBSTITUTIONALLY DISORDERED
SYSTEMS. II. EXPERIMENTAL RESULTS FOR 1,2,4,5-TETRACHLOROBENZENE

D. A. Zwemer and C. B. Harris

Materials and Molecular Research Division
Lawrence Berkeley Laboratory
Department of Chemistry
University of California
Berkeley, California 94720

ABSTRACT

Experimental results for triplet energy partitioning between mobile and stationary states are analyzed in terms of several mechanisms for one-dimensional exciton transfer in substitutionally disordered solids. It is shown that both tunneling and thermal detrapping contribute to triplet exciton mobility under the experimental conditions tested. In addition, singlet exciton migration before intersystem crossing was found to make an important contribution to trap equilibration.

I. INTRODUCTION

The effect of substitutional disorder on energy transfer in molecular crystals has commanded much interest since El-Sayed, Wauk, and Robinson¹ observed the quenching of phosphorescence by chemical impurities. The mediation of trap-trap interactions by the crystal host, as is common in isotopic mixed crystals, has been investigated by observing triplet-triplet annihilation,² delayed fluorescence,³ and energy partitioning between mobile and stationary traps.⁴ Several models have been proposed and experimentally supported to explain long-range exciton transfer between localized trap states. These include quantum tunnelling through virtual states of the host,⁵ thermal detrapping and migration through real states of the host,⁶ and percolation through a continuous trap sublattice in the system.⁴

In the first paper of this series⁷ (referred to as ZH,I), a model for exciton diffusion in a one-dimensional substitutionally disordered system was presented that was based on (i) pure and thermally-assisted tunnelling between trap states in competition with (ii) thermal promotion to the host band and migration to another trap state. Analytic expressions for long-range multi-event exciton transfer across a statistical distribution of one-dimensional trap and host clusters for both models were derived taking the energies and aggregation of the host and trap molecules, the dimensionality of intermolecular interactions, and exciton-phonon coupling into account phenomenologically.

In this paper, we present experimental results for singlet and triplet exciton transfer in a one-dimensional exciton conductor, 1,2,4,5-tetrachlorobenzene, measured by phosphorescence-monitored

energy partitioning between mobile trap states and stationary trap states. We will interpret the concentration and temperature dependence of the partitioning ratio in terms of the models presented in ZH,I. The difference between singlet and triplet exciton migration will be related to the limit of mixed crystal band structure amalgamation.^{8,9}

II. EXPERIMENTAL

A. Sample Preparation and Characterization

The substitutionally disordered one-dimensional band is prepared by isotopic substitution. The perprotonated compound ($\text{h}_2\text{-TCB}$) acts as a trap 22 cm^{-1} below the perdeuterated host molecules ($\text{d}_2\text{-TCB}$), which may also be referred to as the barrier molecules in the limit of high trap mole fraction and low temperature. The energies of the lowest triplet state of the host $\text{d}_2\text{-TCB}$ band and the $\text{h}_2\text{-TCB}$ substituent are determined spectroscopically. The energy of the ${}^3\text{B}_{1\text{u}}$ state of the isolated $\text{h}_2\text{-TCB}$ molecule in the $\text{d}_2\text{-TCB}$ host is also the energy of the center of the ${}^3\text{B}_{1\text{u}}$ $\text{h}_2\text{-TCB}$ band in the neat $\text{h}_2\text{-TCB}$ crystal. The same holds true for the deuterated compound.

The $\text{h}_2\text{-TCB}$ was from Aldrich Chemical and the deuterated compound was prepared as described elsewhere.⁶ A 97.5% deuteration was achieved. Both compounds were zone-refined for 150 passes. The pyrazine was Aldrich Gold Label, 99+%, and used without further purification.

Crystals were grown by standard Bridgeman techniques under carefully standardized crystallization conditions and annealed in their crystal-growing tubes for 10 days at 135°C . The desired proportion of $\text{h}_2\text{-}$ and $\text{d}_2\text{-TCB}$ (m.p. $139.5\text{-}140.5^\circ\text{C}$) was doped with 5% pyrazine (m.p. 54°C), most of which was expelled from the TCB lattice during crystallization and formed a polycrystalline mass on the top of the boule which was discarded.

The relative concentration of $\text{h}_2\text{-}$ and $\text{d}_2\text{-TCB}$ was confirmed by low resolution mass spectra. The pyrazine concentration was below the sensitivity threshold of the mass spectrometer, giving an upper

limit of 0.1 mol%. Comparison of emission for a crystal with low known h₂-TCB fraction in the first series gives a pyrazine mole fraction of 0.0004. The quantity can remain, however, an adjustable parameter. The pyrazine emission is identified by its vibrational structure and the doublet site-splitting of the peaks due to hydrogen bonding onto a neighboring h₂⁺ or d₂-TCB molecule.¹⁰ The hd-TCB trap, although present in concentrations up to 4 mol%, is rapidly depopulated by thermal promotion and is not observed. In pure h₂-TCB crystals, both h₂-TCB exciton emission and x-trap emission is observed. The x-trap is 40 cm⁻¹ below the band and it can in all likelihood be ascribed to a mechanical defect in the lattice along a dislocation plane, although the exact nature of the state is unknown. The x-trap was treated as an additional stationary trap whose concentration remained a constant fraction of stationary trap emission.

B. Sample Excitation

The phosphorescent triplet state was excited directly with a Molelectron UV1000/DL300 nitrogen-laser-pump dye laser with PBD (Eastman Kodak, λ_{max} 380 nm) in dioxane undoubled. In these experiments, the h₂-TCB triplet vibronic origin was pumped, having been identified by a phosphorescence monitored excitation spectrum. The singlet state was excited with a broadband H_g lamp with Schott 2800 HÅ UV interference filter. The crystal samples were mounted in a cryogenic dewar in contact with liquid helium whose temperature could be maintained between 4.2°K and 1.4°K by pumping. Phosphorescence at right angles to the excitation source was focused on the slits of a Spex 3/4 m spectrometer and detected with an EMI 6256 photomultiplier tube. All vibronic

peaks for the first 200 Angstroms beyond the triplet origins were measured from the original spectra by peak height and halfwidth.

Due to the pulsed nature of the dye laser triplet excitation, several experiments were repeated to confirm that different laser repetition rates and detector time constants did not effect the energy partitioning ratios. Experiments were also repeated with neutral density filters between laser and crystal, showing only linear changes in phosphorescence intensity. Non-linear effects were therefore presumed to be insignificant. Laser emission was not strongly polarized and crystals were mounted with the c axis perpendicular to both excitation and detection axes, so polarization effects were not considered.

III. RESULTS AND DISCUSSION

A. One-Dimensional System

The system we have chosen for this investigation, 1,2,4,5-tetrachlorobenzene (TCB), has been shown^{11,12} from a variety of criterion to be almost exclusively one-dimensional in its triplet band along a translationally equivalent axis. The tetrachlorobenzene crystal structure¹³ is such that the stacking along the \underline{c} axis with the planes of the aromatic rings parallel to one another at an angle of 66° to the \underline{c} axis. This is illustrated in Fig. 1. The adjacent molecules are separated by 3.86Å along the \underline{c} axis although the distance between molecules along an axis normal to the planar benzene rings is only 3.53Å. Translationally equivalent molecules along the other axes are separated by 9.6Å and 10.5Å. As a result of the structure, the largest intermolecular interaction, β_c , in the ${}^3B_{1u}$ triplet state is along \underline{c} . It has been shown that the triplet band along \underline{c} is ~ 1.25 cm^{-1} wide¹⁴ while that associated with the translationally non-equivalent molecules is less than 10^{-5} cm^{-1} .¹¹ To a first approximation then, the ratio of the translationally equivalent to nonequivalent interactions is greater than 10^5 to 1 and one expects the system to be accurately described by a one-dimensional band structure in the triplet manifold. The important energy levels are shown schematically in Fig. 2.

B. Triplet Excitation

The ratio of stationary trap phosphorescence to total phosphorescence for direct triplet excitation into the $h\nu$ -TCB band is plotted against $h\nu$ -TCB mole fraction in Fig. 3. The x-trap comprises a constant percentage ($\pm 5\%$) of the stationary trap phosphorescence. Preliminary

work at 1.4°K has shown an absence of stationary trap phosphorescence below $x_h = 0.50$ and a gradual increase to include all emission at $x_h = 1.0$.¹⁵ For the region above $x_h = 0.60$, Fig. 3 shows that stationary trap phosphorescence increases regularly with mobile trap concentration and temperature. The temperature dependence for each crystal is plotted in an Arrhenius-type plot in Fig. 4, where it shows a linear dependence with a different activation energy at each concentration.

The delayed onset of pyrazine phosphorescence is strong confirmation of the one-dimensional nature of the intermolecular interaction. Percolation theory states that an unblocked site probability (corresponding to a mobile trap probability in this context) of 50% in a two-dimensional rectangular lattice and 25% in a cubic lattice will establish a complete network of adjacent trap states within a macroscopic sample.¹⁶ The rapid communication between trap sites in such a network would enable the h_2 -TCB trap to populate the stationary states within the triplet state lifetime. Such behavior has been observed in naphthalene, a two-dimensional exciton conductor, although the sharp transition between mobile trap and stationary trap emission occurs well below the predicted 50% threshold due to long-range tunnelling between traps or a small intermolecular interaction along the third crystal axis.⁴

In ZH,I, we proposed two models to describe exciton migration in a one-dimensional isotopically disordered system in the narrow bandwidth limit. We have attempted to fit the experimentally observed phosphorescence intensity distribution of Fig. 3 to the trap population distributions calculated for the detrapping and tunnelling models.

Most model parameters, including triplet state lifetime T , intermolecular interaction β , isotopic splitting Δ , and pre-exponential detrapping frequency H , have been evaluated in previous work.^{5,6,11} Only the stationary trap concentration x_s could not be accurately obtained.

The thermally-assisted tunnelling model proposes that exciton transfer takes place exclusively along the one-dimensional chain in a random walk between mobile trap states by tunnelling through host molecule barriers. The tunnelling rate through a barrier n molecules wide, $k(n)$, falls with increasing barrier width n and trap depth Δ

$$k(n) = 4\beta^{n+1}/\Delta^n h \quad (1)$$

and above a certain width, the barriers may be treated as impenetrable during the excited state lifetime. Transmission is dependent on temperature because tunnelling may take place from a state thermally promoted above the mobile trap origin. Because of the n^{th} power dependence of the tunnelling rate on Δ , a small decrease in Δ may greatly increase the average thermally-assisted tunnelling rate

$$\langle k(n) \rangle_\epsilon = \int_0^{\Delta-\delta} \left[\frac{h}{4\beta^{n+1}} (\Delta - \epsilon)^n \right]^{-1} e^{-\epsilon/kT} d\epsilon / \int_0^{\Delta-\delta} e^{-\epsilon/kT} d\epsilon \quad (2)$$

where ϵ is the energy of the phonon-exciton complex above the mobile trap origin and the constraint $\Delta \gg \delta \gg \beta$ insures that the average will not be carried over a region where Eq. (1) breaks down. This formulation of the tunnelling model holds only in the limit $kT \ll \Delta$. The population distributions in Fig. 5 are calculated for a random walk over a statistical distribution of barriers. Salient features are a roughly linear concentration dependence on x_{mob} , the mobile

trap mole fraction, in the threshold region, a weak temperature dependence below 2.4°K, and a concentration dependent activation energy.

Figure 6 shows the corresponding curves generated for the thermal detrapping model, where barrier transmission occurs by thermal promotion of an exciton from a mobile trap state to the host barrier states and subsequent migration along the one-dimensional chain to another trap site. The probability of migration to a new site relative to retrapping at the original site is accounted for by the migration efficiency α . The barrier transmission rate is the product of the detrapping rate $K_{\epsilon k}$ and the migration efficiency α averaged over the statistical distribution of barrier widths,

$$K_{\epsilon k} = N e^{-\Delta/kT} \quad (3)$$

$$\langle \alpha \rangle = \frac{1-x}{x^2} \left[\ln \left(\frac{1}{1-x} \right) - 1 \right] \quad (4)$$

Exciton migration is again treated as a random walk with a barrier density set by the mobile trap density. The important features of Fig. 6 are the strong temperature dependence and the weak concentration dependence over much of the range.

The most important observation to be drawn from Figs. 4 and 5 is that both models predicted significant exciton mobility under the experimental conditions studied. Neither mechanism is individually sufficient to predict the experimental results. At the lowest temperatures reached, tunnelling is the predominant barrier transmission process and experimental results in Fig. 7 match the gradual onset

of stationary trap phosphorescence starting about $x_{\text{mob}} = 0.50$ that is characteristic of the tunnelling model. As the sample temperature increases, detrapping surpasses tunnelling as the major transmission process. The detrapping model predicts almost complete Boltzmann thermalization at 4.2°K between stationary and mobile trap states, which is seen experimentally in Fig. 8. The results of the experiments confirm the salient features of the theory (ZH,I) and show that a thorough treatment of triplet exciton dynamics in disordered systems must address itself to both mechanisms.

C. Singlet Excitation

The same system under singlet excitation shows important differences in behavior. Figure 9 shows the fraction of stationary trap phosphorescence for singlet excitation. The differences between this graph and Fig. 3 shows that significant exciton migration and trapping occur in the singlet manifold before intersystem crossing into the triplet.

The bandwidth of singlet excited states is generally orders of magnitude larger than the triplet bandwidth, but these singlet state lifetimes are relatively so short that exciton migration is considered primarily a triplet state phenomenon in many systems. The singlet bandwidth may play a critical role, however, in substitutionally disordered crystals. The TCB triplet bandwidth, about 1.2 cm^{-1} , is much smaller than the 23 cm^{-1} isotope shift and the triplet bands are an example of the persistence limit. Neither the isotopic shift nor the bandwidth are known for the first excited singlet state, but phosphorescence monitored absorption spectroscopy performed by scanning the excitation source across the singlet absorption near 2965 \AA indicated

a bandwidth greater than 100 cm^{-1} if transitions to the entire band are allowed by disorder induced mixing of k states. It is reasonable that the singlet isotope shift is comparable to the bandwidth and the d_2 - and h_2 -TCB singlet bands are amalgamated^{8,9} over the whole concentration range. The nearest pyrazine singlet state is 2700 cm^{-1} lower and does not take part.

The composition of the supertrap phosphorescence is significantly different between the singlet and triplet data. For triplet excitation, x-trap phosphorescence comprises $\sim 55\%$ of all supertrap emission, while in the singlet it accounts for only 5-10%. This may be explained if the x-trap does not act as a trap in the excited singlet state or is masked by the increased bandwidth. The x-trap phosphorescence then gives us a measure of how many excitons are trapped after inter-system crossing to the triplet and therefore how many are trapped in the singlet. By this measure, 75-80% of the total phosphorescence is due to trapping at a pyrazine from the singlet state and this quantity is independent of the composition of the crystal. In Fig. 10, a constant 80% of the pyrazine phosphorescence at 1.7°K in Fig. 9 has been subtracted out and the remainder normalized to 100%. The result is identical within experimental error to the triplet result. The important conclusions are that exciton migration in excited singlet states may be comparably efficient with that in much longer-lived triplet states in disordered crystals and that energy transfer through an amalgamated band is independent of the band composition.

IV. SUMMARY

(i) We have presented experimental energy-partitioning data between mobile and stationary trap states along a one-dimensional exciton conductor for both singlet and triplet excitation. The percentage of stationary trap phosphorescence increases with increasing mobile trap concentration, with increasing temperature, and is larger for singlet excitation than for triplet excitation.

(ii) Two simple models for (i) resonant tunnelling transfer and (ii) thermal detrapping and migration across a statistical distribution of barriers, do not, on an individual basis, accurately represent the experimental results for triplet excitation. Both mechanisms are important and contribute to exciton mobility over the temperature range studied.

(iii) Where competition between singlet and triplet manifolds for exciton migration occurs, the singlet may be much less efficient in the unperturbed crystal because of its short lifetime. In a substitutionally disordered crystal, the much wider bandwidth of the singlet may hide the perturbation of the potential surface and allow much more efficient exciton transfer than the triplet. The experimental data presented here shows that ~80% of the excitons reach a supertrap in the singlet state before intersystem crossing and that this percentage is independent of the band composition.

ACKNOWLEDGEMENT

This work was supported by the Division of Chemical Sciences,
Office of Basic Energy Sciences, U. S. Department of Energy.

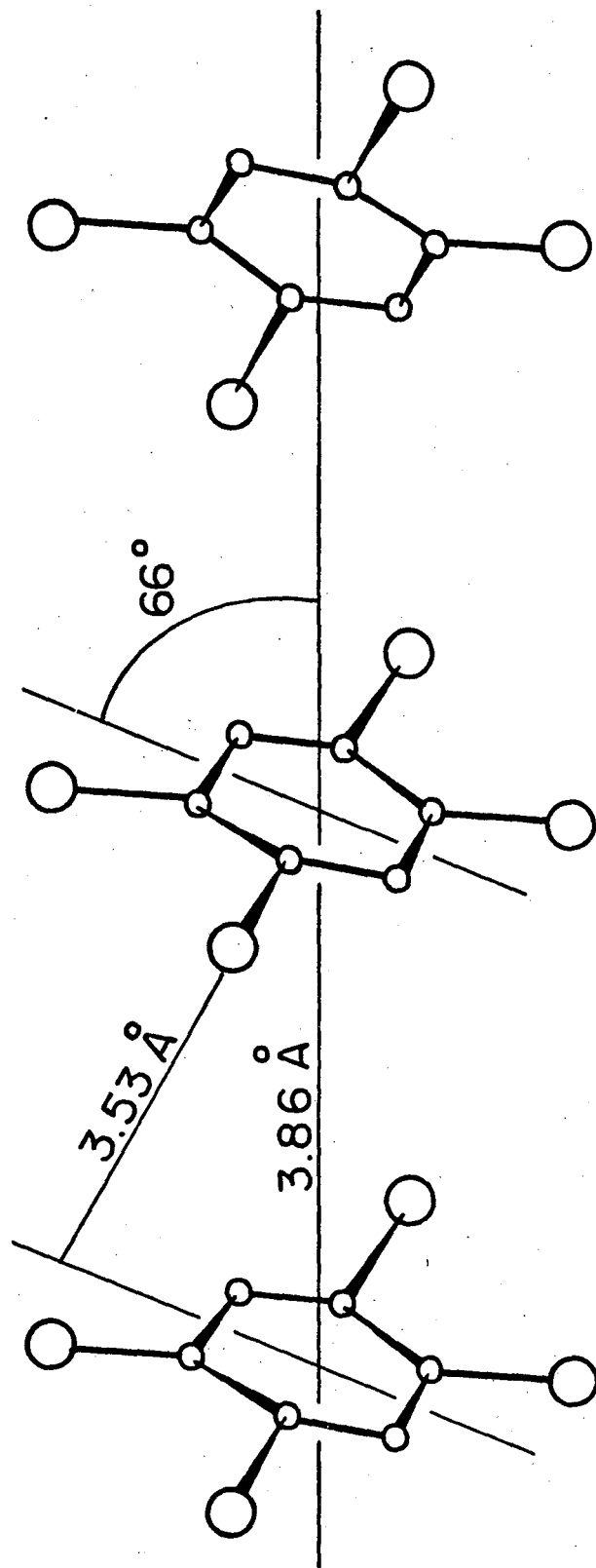
REFERENCES

1. M. A. El-Sayed, M. T. Wauk, and G. W. Robinson, *Mol. Phys.* 5, 205 (1962).
2. H. Sternlicht, G. C. Nieman, and G. W. Robinson, *J. Chem. Phys.* 38, 1326 (1963).
3. P. Avakian and R. E. Merrifield, *Mol. Cryst.* 5, 37 (1968).
4. R. Kopelman, E. M. Monberg, F. W. Ochs, and P. N. Prasad, *J. Chem. Phys.* 62, 292 (1975).
5. M. T. Lewellyn, A. H. Zewail, and C. B. Harris, *J. Chem. Phys.* 63, 3687 (1975).
6. M. D. Fayer and C. B. Harris, *Chem. Phys. Lett.* 25, 149 (1974).
7. D. A. Zwemer and C. B. Harris, *J. Chem. Phys.* 68, 2184 (1978).
8. Y. Onodera and Y. Toyozawa, *J. Phys. Soc. Japan* 24, 341 (1968).
9. J. Hoshen and J. Jortner, *J. Chem. Phys.* 56, 5550 (1972).
10. E. F. Zalewski and D. S. McClure, in Molecular Luminescence, E. C. Lim, ed. (W. A. Benjamin, 1969), p. 739.
11. A. H. Francis and C. B. Harris, *Chem. Phys. Lett.* 9, 181,188 (1971).
12. A. H. Zewail and C. B. Harris, *Phys. Rev. B* 11, 952 (1975).
13. F. H. Herbstein, *Acta Cryst.* 18, 997 (1965).
14. D. D. Dlott and M. D. Fayer, *Chem. Phys. Lett.* 41, 305 (1976).
15. D. A. Zwemer and C. B. Harris, unpublished results.
16. V. K. Shante and S. Kirkpatrick, *Adv. Phys.* 20, 325 (1971).

FIGURE CAPTIONS

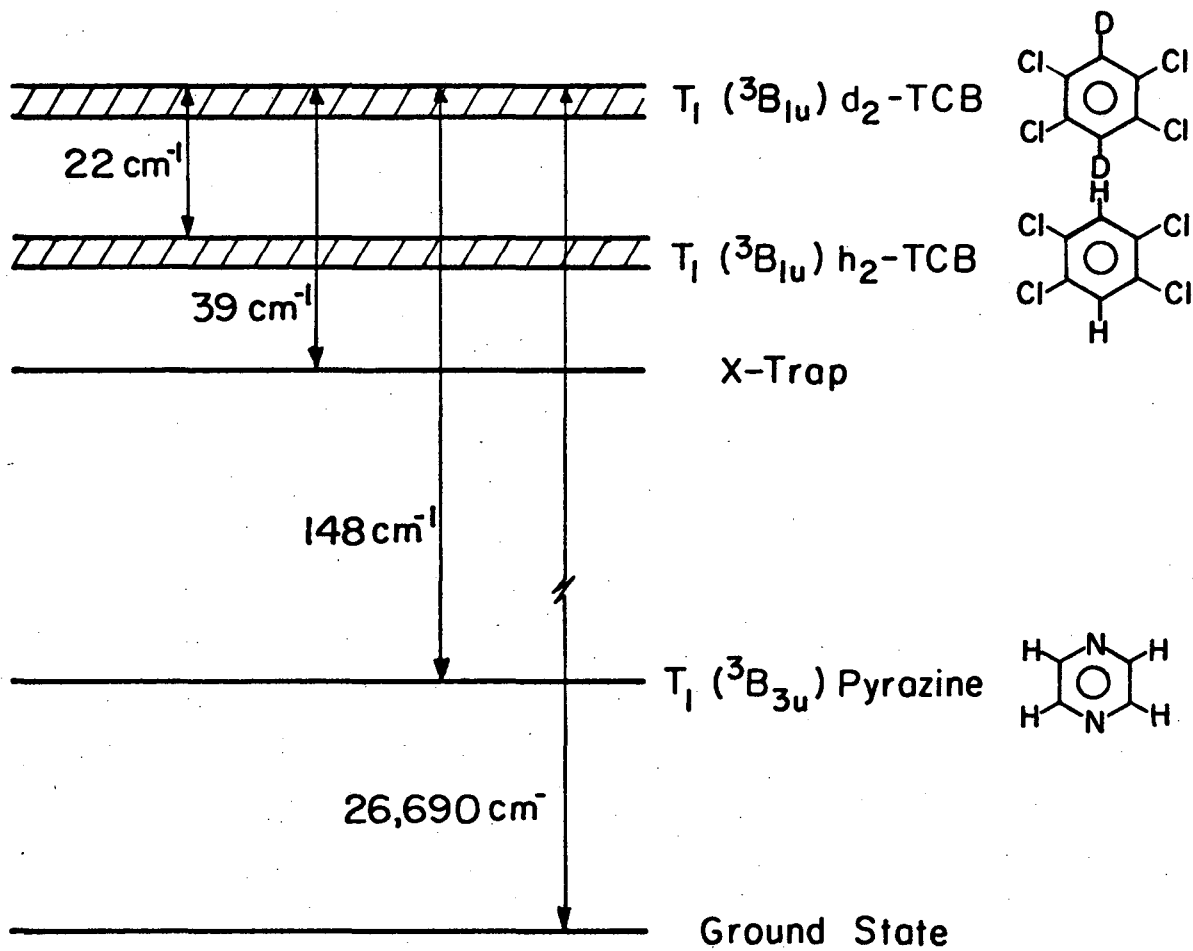
- Fig. 1. Translationally equivalent TCB molecules along c-axis show maximum π -electron overlap.
- Fig. 2. Schematic of relevant energy levels of ternary TCB-pyrazine system. Pyrazine and x-trap constitute $<0.1\%$. TCB bandwidth is 1.2 cm^{-1} .
- Fig. 3. Ratio of stationary trap (pyrazine and x-trap) phosphorescence intensity to total phosphorescence intensity vs. x_{mob} , the mole fraction of h_2 -TCB, the mobile trap. Dotted lines show linear least squares fit to experimental points.
- Fig. 4. Ratio of stationary trap phosphorescence to total phosphorescence vs reciprocal temperature. Solid lines are least squares fits for different crystals identified by h_2 -TCB mole fraction at right. The activation energies are 2.4 cm^{-1} for $x_{\text{mob}} = 0.60$, 1.7 cm^{-1} for $x_{\text{mob}} = 0.70$, 0.84 cm^{-1} for $x_{\text{mob}} = 0.80$, 0.24 cm^{-1} for $x_{\text{mob}} = 0.90$, and 0.19 cm^{-1} for $x_{\text{mob}} = 0.95$.
- Fig. 5. Calculated population partitioning ratio for thermally-assisted tunnelling transfer vs h_2 -TCB mole fraction between 1.4 and 4.2 K. Parameter values are $T = 25 \text{ msec}$, $\beta = 0.3 \text{ cm}^{-1}$, $\delta = 1/2\Delta$ and $x_s = 0.002$. Maximum penetrable barrier is 4 d_2 -TCB molecules wide.
- Fig. 6. Calculated population partitioning ratio for thermally detrapping exciton transfer vs h_2 -TCB mole fraction between 1.4 and 4.2 K. Parameter values are $T = 25 \text{ msec}$, $\beta = 0.3 \text{ cm}^{-1}$, $x_s = 0.002$, and $H = 3 \times 10^{10} \text{ sec}^{-1}$.

- Fig. 7. Comparison of experimental intensity partitioning ratio (open circles) with predicted population partitioning ratios for tunneling (solid line) and detrapping (dashed line) at 1.78 K. Curves are taken from Figs. 4-6.
- Fig. 8. Comparison of experimental intensity partitioning ratio (open diamonds) with predicted population partitioning ratios for tunneling (solid line) and detrapping (dashed line) at 4.2 K. Curves are taken from Figs. 4-6.
- Fig. 9. Experimental values for ratio of stationary trap phosphorescence to total phosphorescence for singlet excitation vs h_2 -TCB (mobile trap) mole fraction, x_h , at 1.4 K.
- Fig. 10. Comparison of triplet excited phosphorescence ratios (dark circles, left hand scale) with singlet excited phosphorescence ratios (open circles, right hand scale) vs h_2 -TCB mole fraction at 1.4 K.



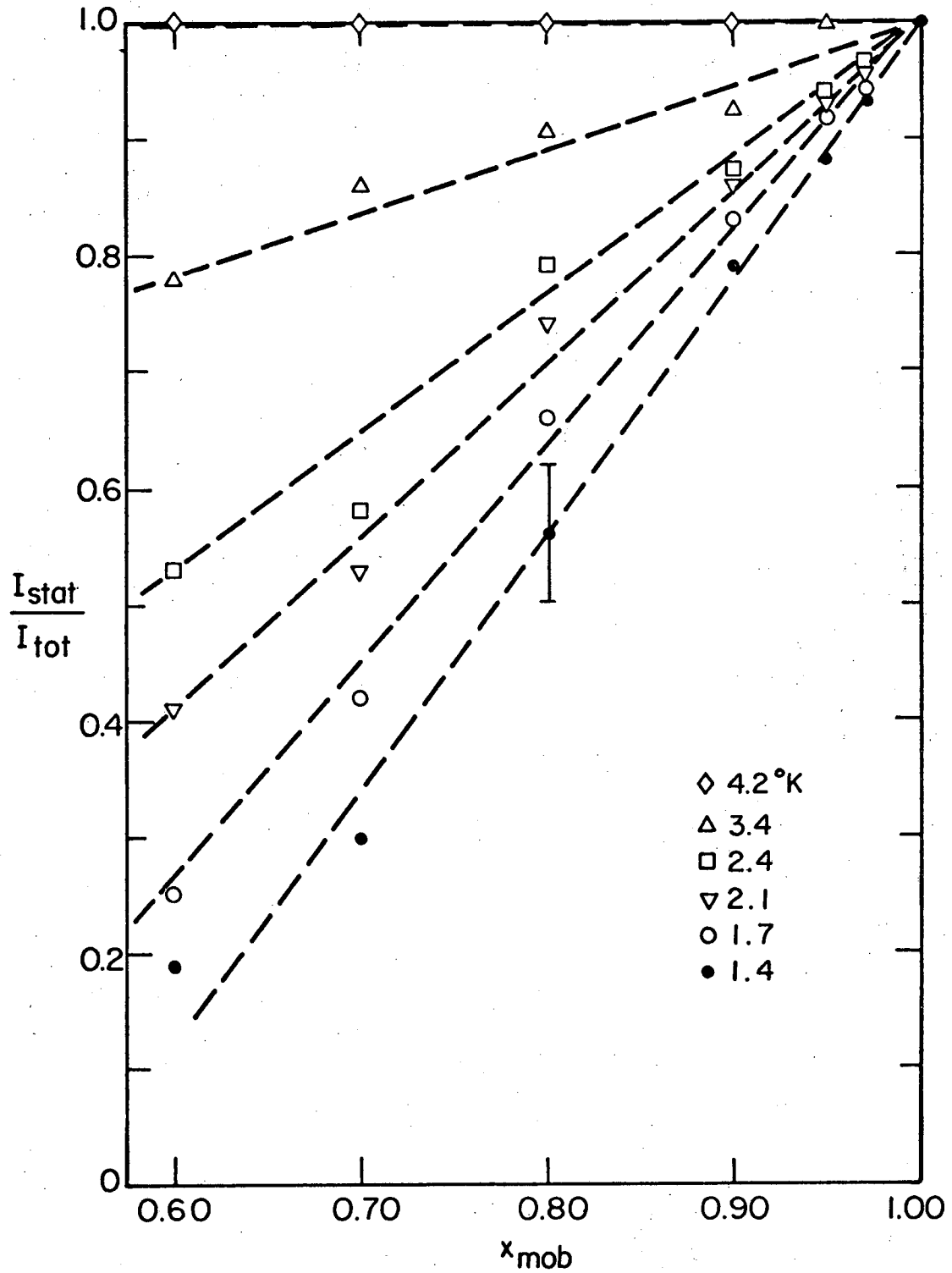
XBL 766-7104

Figure 1



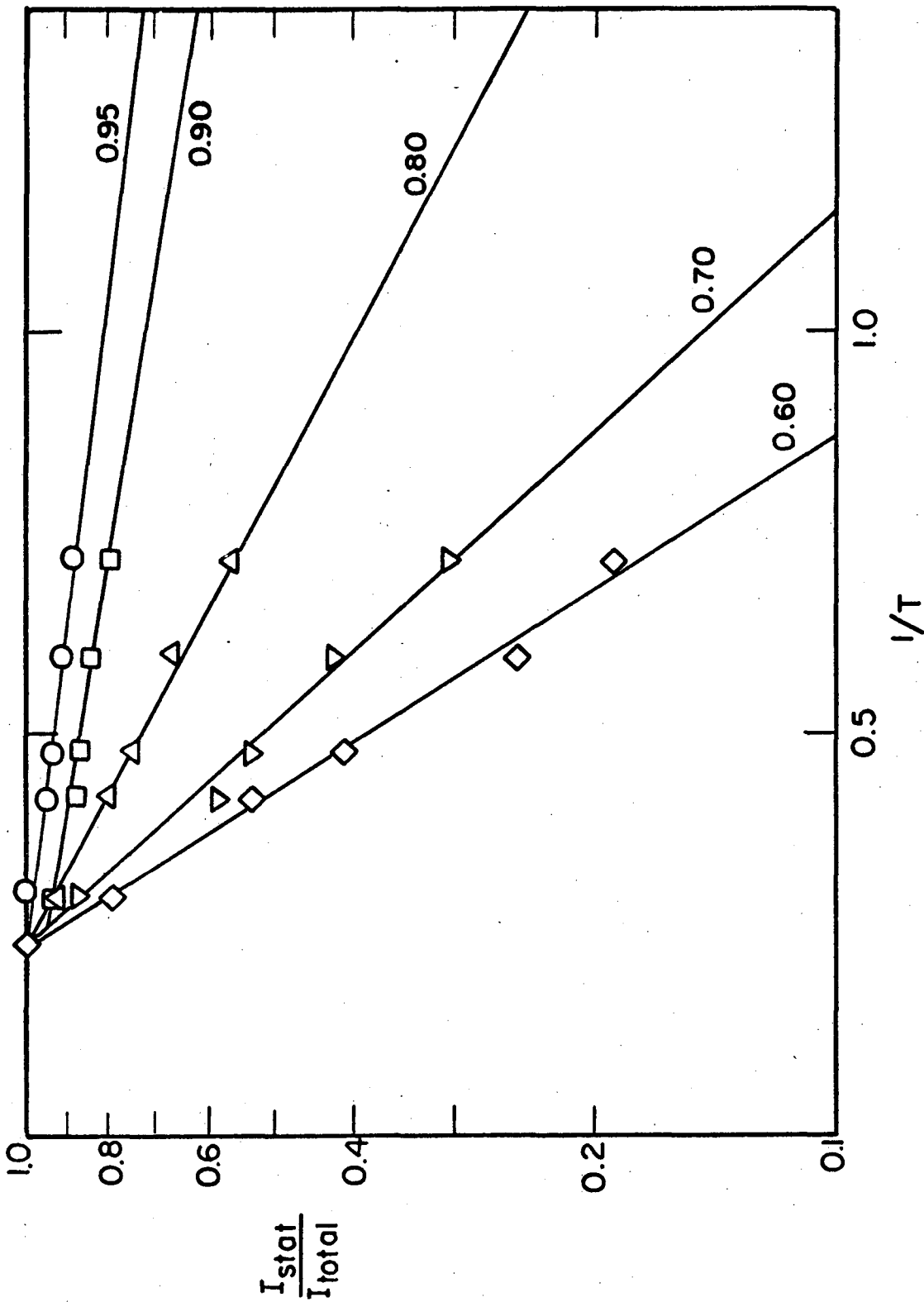
XBL766-7105

... Figure 2



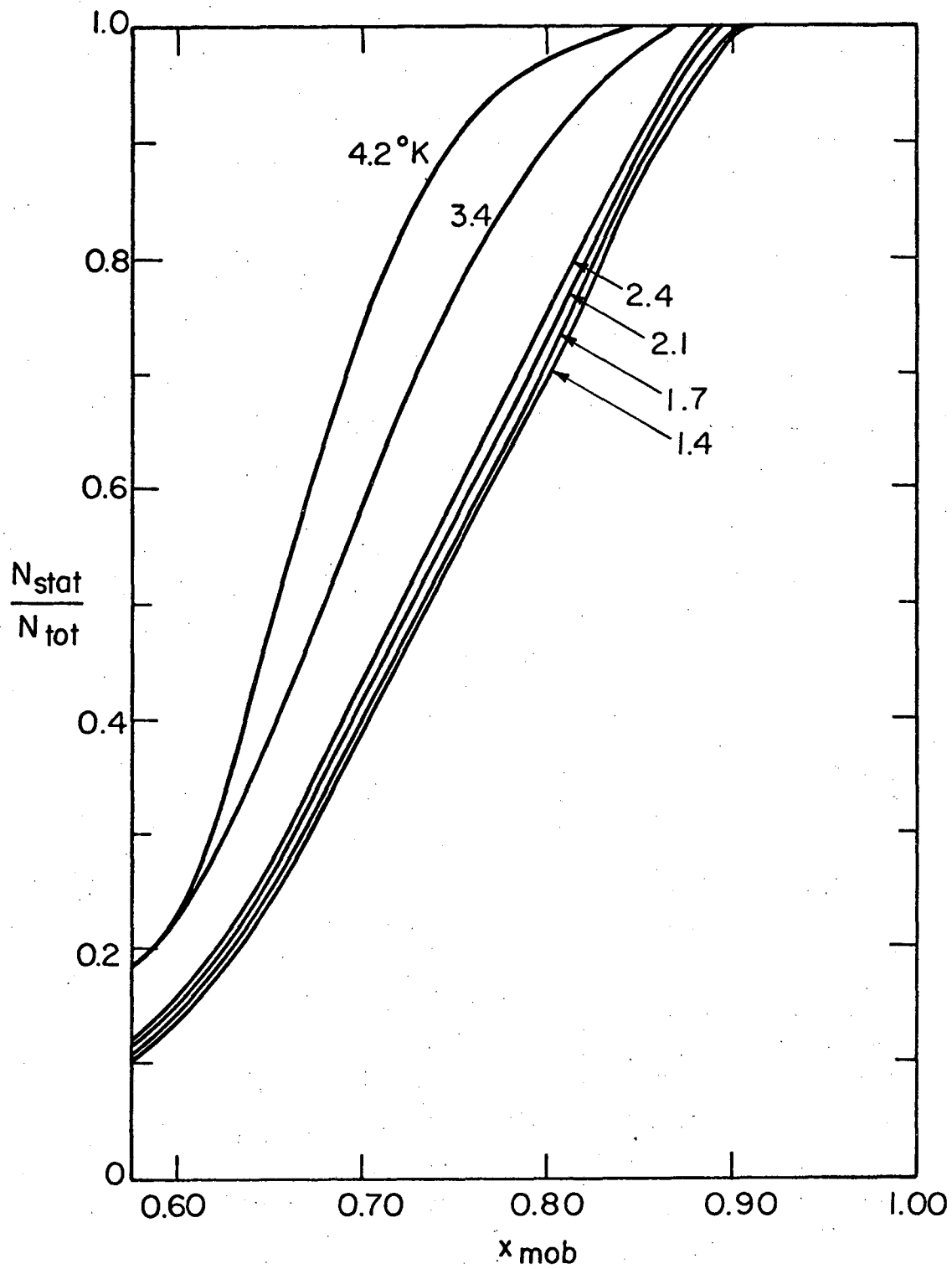
XBL 772-5099

Figure 3



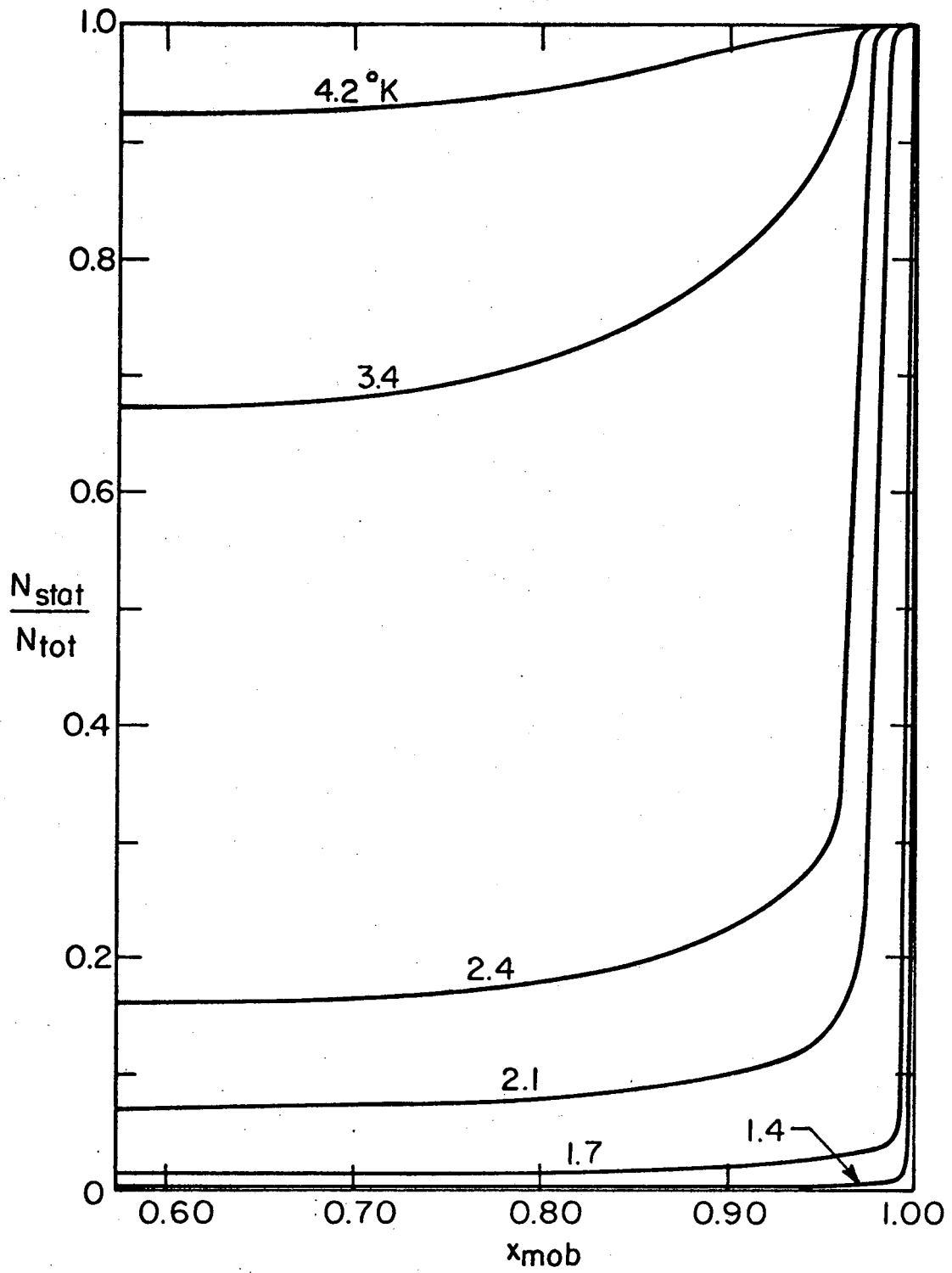
XBL 766-7111

Figure 4



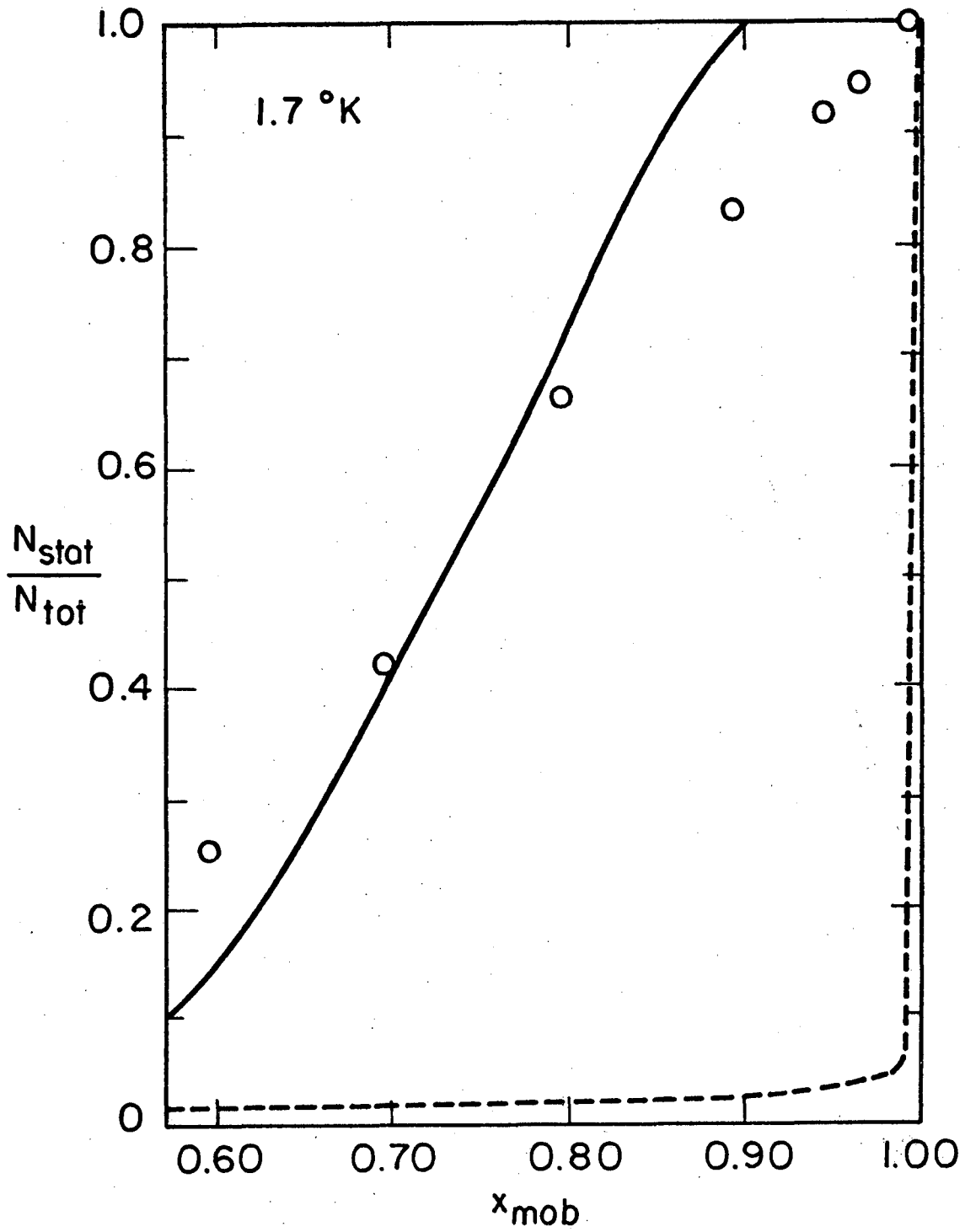
XBL 772-5101

Figure 5



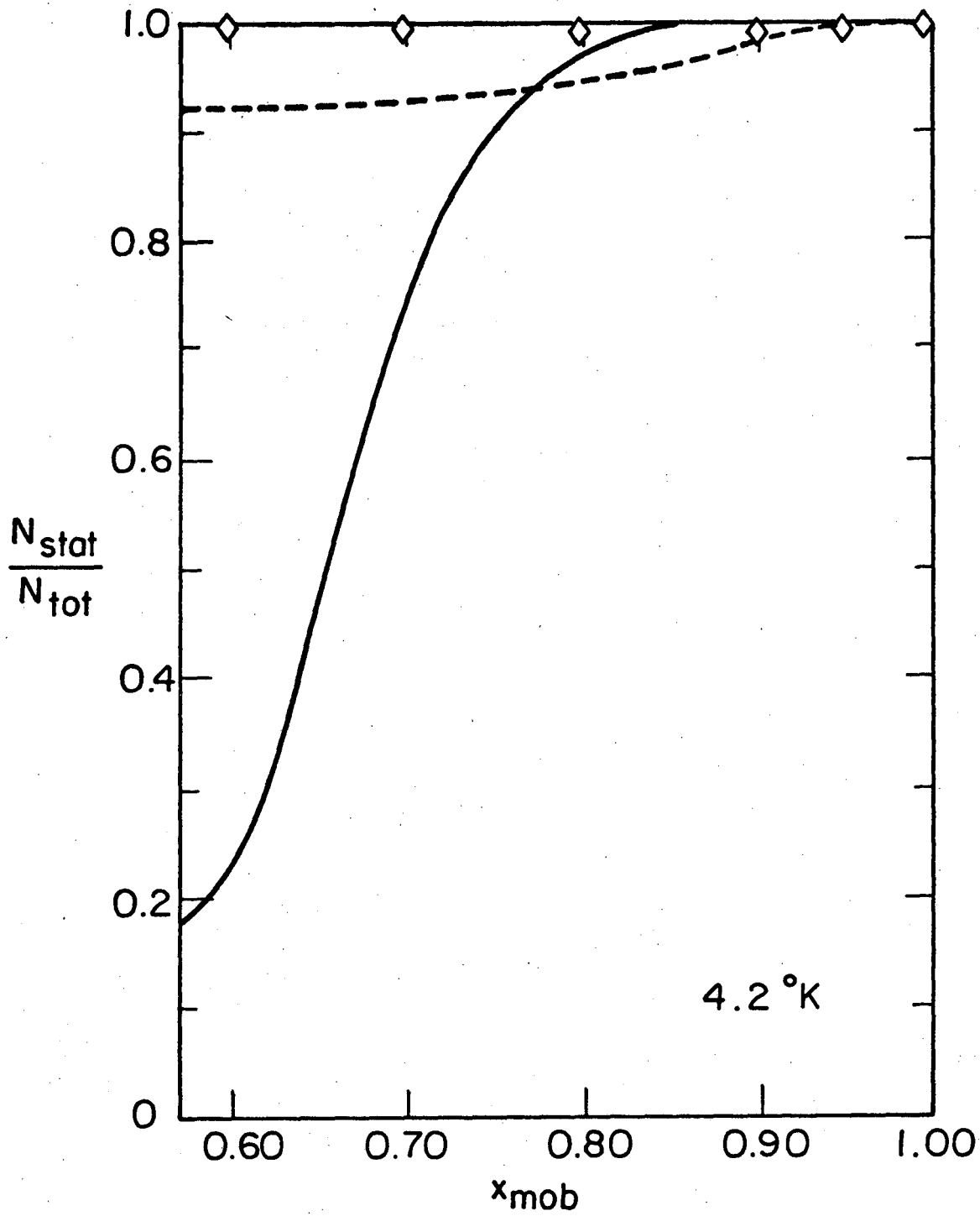
XBL772-5100

Figure 6



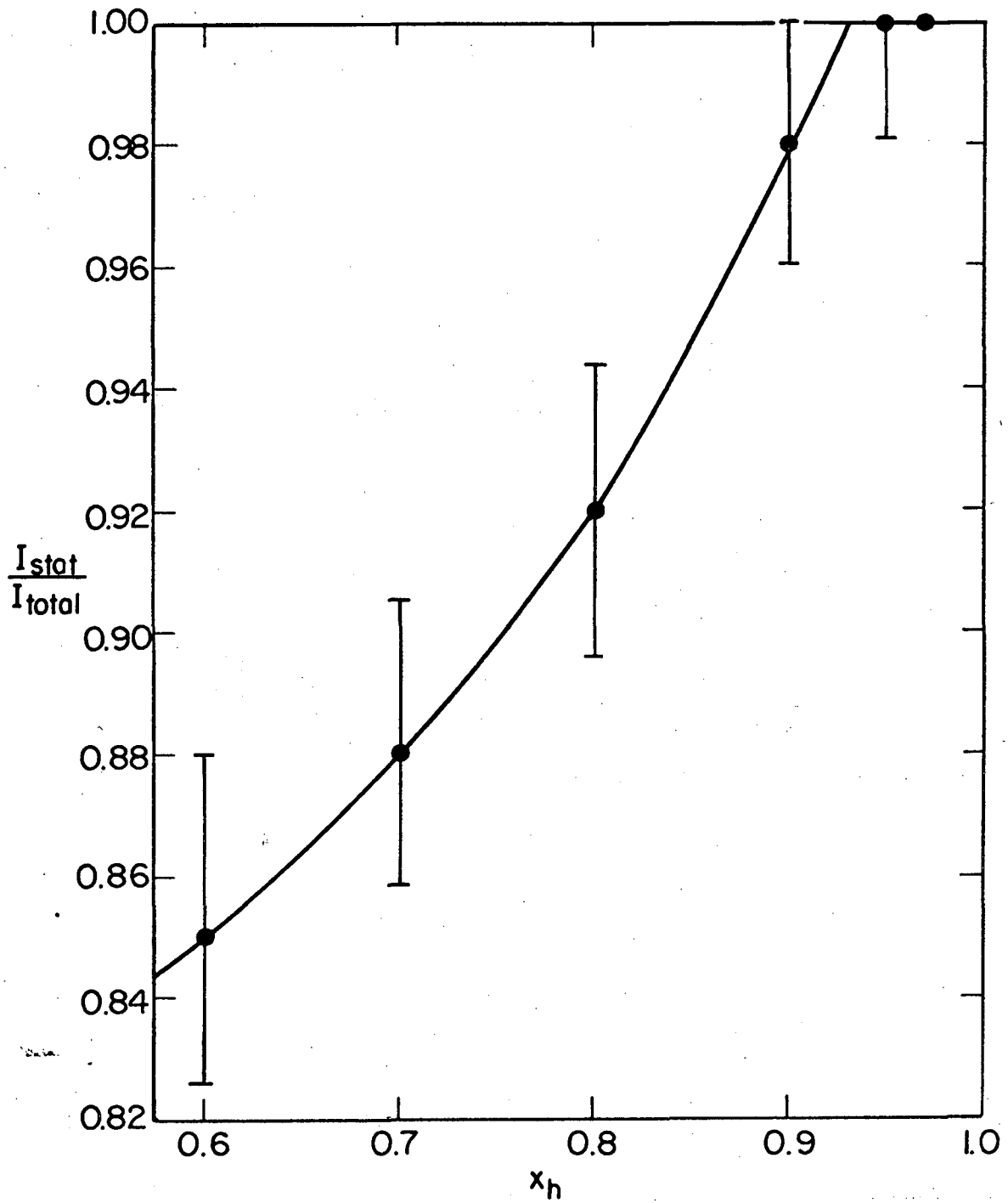
XBL784-4834

Figure 7



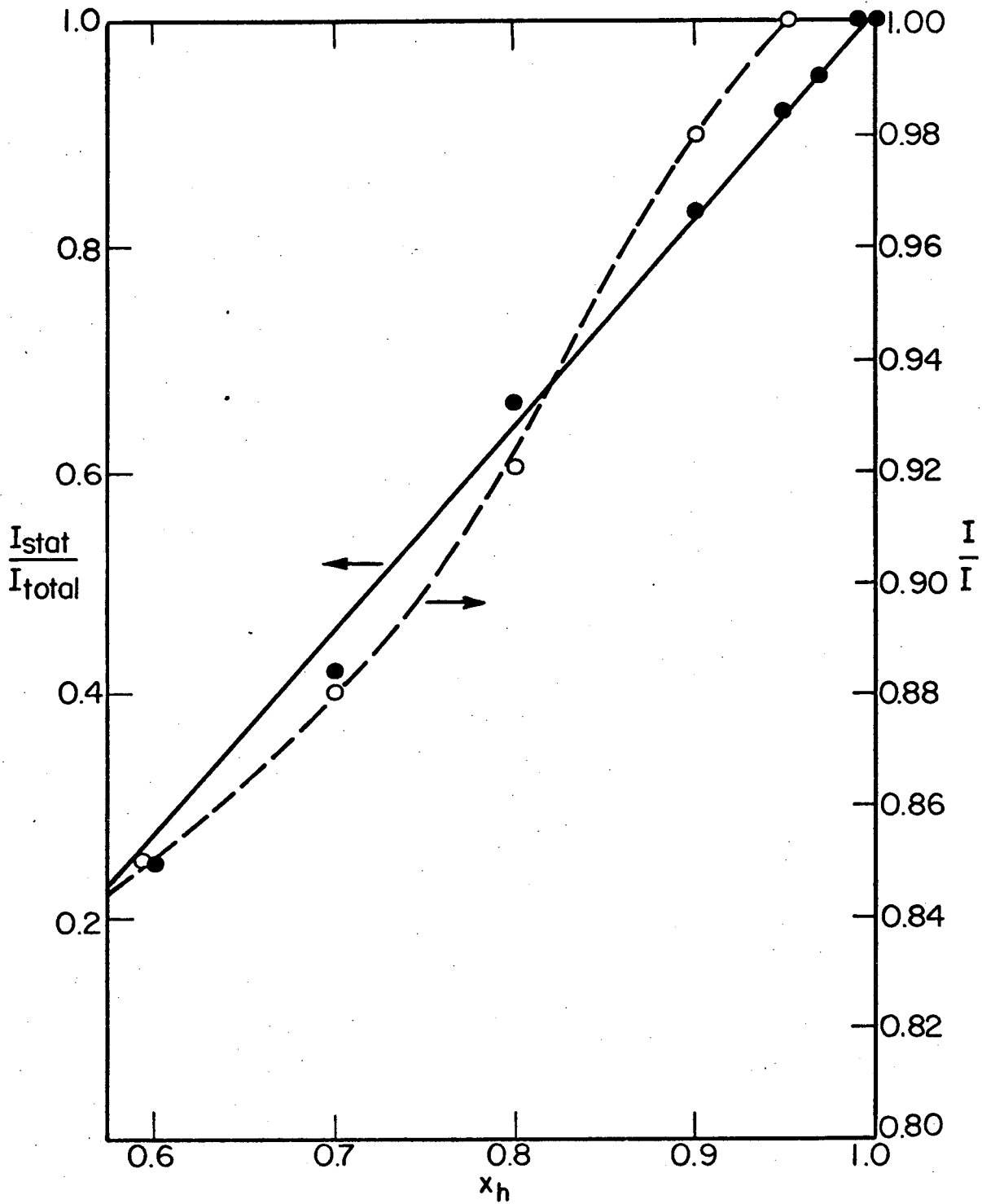
XBL 784- 4835

Figure 8



XBL 766-7108

Figure 9



XBL 766-7116

Figure 10

This report was done with support from the Department of Energy. Any conclusions or opinions expressed in this report represent solely those of the author(s) and not necessarily those of The Regents of the University of California, the Lawrence Berkeley Laboratory or the Department of Energy.

TECHNICAL INFORMATION DEPARTMENT
LAWRENCE BERKELEY LABORATORY
UNIVERSITY OF CALIFORNIA
BERKELEY, CALIFORNIA 94720